

Share Your Innovations through JACS Directory

Journal of Advanced Chemical Sciences

Visit Journal at http://www.jacsdirectory.com/jacs



Ceramic Waste-Based Natural Rubber Composites: An Exciting Way for Improving Mechanical Properties

Y.G. Kondarage¹, H.M.J.C. Pitawala¹, T. Kirushanthi¹, D. Edirisinghe², Thusitha N. Etampawala^{3,*}

- ¹Department of Science & Technology, Faculty of Science & Technology, Uva Wellassa University, Sri Lanka.
- ²Department of Rubber Technology and Development, Rubber Research Institute, Sri Lanka.
- ³Instrument Centre, Faculty of Applied Sciences, University of Sri Jayewardenepura, Sri Lanka.

ARTICLE DETAILS

Article history:
Received 19 August 2018
Accepted 08 September 2018
Available online 19 September 2018

Keywords: Ceramic Waste Surface Modification Rubber Composite Reinforcement of Rubber

ABSTRACT

Large amounts of fired ceramic waste produced in ceramic industry do not have a proper method to reuse and mainly thrown away into landfills since fired ceramics have already been sintered and thus their utilization as a raw material is limited. However, these solid wastes have a major environmental and economic concern. Thus, a proper management of such solid wastes is eminent. This research is dedicated to evaluating the possibility of using such ceramic waste as a low-cost filler material in the manufacture of natural rubber based composites. Ceramic particles smaller than 125 μm were selected initially for the preparation natural rubber based composites. For the latter part of the study, particles in sub-micrometer length scales were used. Elemental analyses and composition of the phases of the ceramic particles were determined by X-ray fluorescence and diffraction respectively. The average particle size was characterized by scanning electron microscope (SEM). The surfaces of the sub micrometer size ceramic particles were modified using Silane69 coupling agent. The surface modification was confirmed by Fourier-transform infrared spectroscopy, thermo gravimetric analysis and SEM coupled with energy-dispersive X-ray spectroscopy. Natural rubber based composites were prepared with different levels of ceramic filler loadings. The mechanical properties of the composites such as hardness, resilience, compression set, abrasion volume loss and tensile properties were evaluated. These properties of the composites were compared with those of the composites prepared according to the same formulation except the ceramic filler (control). The composites were found to have an exciting enhancement of mechanical properties with respect to the control. The mechanical property improvement is higher when the ball milled sub-micrometer size ceramic filler is used and it is even better when surface modified ceramic particles are used.

1. Introduction

An increase in the generation of different type of wastes can be observed due to the industrialization and rapid economic growth in recent decades [1]. Current practices in dumping or destroying waste in industries have badly affected in the natural environment including water, soil, air and noise pollution [1,2]. At the same time, these practices represent an economic cost. If waste is managed correctly it can be converted into a useful resource, which contributes to savings in raw materials, conserve action of natural resources and the climate, and promotes sustainable development [3].

According to the predicted statistics about 19 billion tons of solid wastes are expected to be generated annually by the year 2025 [2]. Annually, Asia alone generates 4.4 billion tons of solid wastes. A high demand, scarcity of raw materials, and high price of energy the cost of construction materials is increasing day by day [3]. So the use of alternative constituents in construction materials has now become a global concern [4-7]. If these ceramic wastes are utilized to re-use in industry, it will minimize the cost for raw materials and minimize the environmental pollution [3, 4].

The ceramics industry is mainly comprised of the following subsectors: wall and floor tiles, sanitary ware, bricks and roof tiles, refractory materials, technical ceramics and ceramic materials for domestic and ornamental use [4]. It was observed that ceramic wastes are the kind of major wastes in manufacturing sectors. Ceramic wastes are produced as a result of the ceramic processing. These wastes cause soil, air, and groundwater pollution. The main problem which ceramic waste inheriting

is they are already sintered and cannot be easily reused due to their irreversible phase transition during the processing [8-10].

In this research work ceramic wastes from floor tiles and sanitary wares were planned to be composited with natural rubber latex.

Natural rubber has properties of plasticity or viscosity, elasticity, tensile strength. However, to improve the quality of the rubber several kinds of fillers are added to the natural rubber matrix [11]. The reinforcing fillers significantly increase or maintain the strength of rubber composites, while the non-reinforcing fillers are helpful in reducing the cost [12, 13]. Ceramic waste can be used to replace the fillers such like silica and carbon black. The filler compatibility in rubber composites depends on particle size, the structure of filler particles, and surface activity [12, 13]. Fillers which contain chemically active surfaces from various chemical groups facilitate better interaction between rubber and filler by the formation of strong covalent bonding. The hydrophobic and hydrophilic nature of rubber and filler also influence the compatibility and dispensability of filler in the rubber matrix.

In this research waste ceramic was crushed and it was used as the filler material with natural rubber. Natural rubber so called cis-poly isoprene is a non-polar substance [14-16]. To overcome this polarity mismatch, the surface of the ceramic waste powder was modified using Silane69 (bis (3-triethoxysilylpropyl) tetrasulfane) coupling agent. In order to provide more available contact between the rubber molecule and the filler particle, the particle size of ceramic particles were greatly reduced. We have observed interesting results with different loadings of surface modified ceramic powders.

^{*}Corresponding Author:tetampa@sjp.ac.lk(Thusitha N. Etampawala)

2. Experimental Methods

2.1 Preparation of Ceramic Waste Powder and Characterization

Ceramic floor tile waste and sanitary ware waste were collected from manufacturing sectors and domestically. Those waste were crushed and grinded using a mechanical method. Then the crushed ceramic wastes were sieved using mechanical sieve shaker (Aimil Ltd., India) and particles size less than $125~\mu m$ were obtained.

In the preparation of sub micrometer sized ceramic waste powder, Initially prepared ceramic waste powder was ball milled for 6 hours at an 800 rpm speed by a laboratory planetary ball mill (TENCAN, China) followed by dry milling [17-19].

Fourier transform infrared (FTIR) spectra of KBr pellets prepared from this initial ceramic powder were obtained using FTIR spectrophotometer (Bruker, USA). Elemental analyses and composition of the phases of these initial ceramic particles were determined by X-ray fluorescence spectrometer and X-ray diffractometer (Rigaku Ultima IV, USA) respectively. The average particle size was characterized by scanning electron microscope (EVOLS15, Germany).

2.2 Surface Modification of Ceramic Particles and Characterization

Ceramic powder surfaces were modified with Silane69 coupling agent with slight modifications of the methods followed by Wu et al. [16]. Firstly, $10\,\mathrm{g}$ of ceramic powder was added to an appropriate amount of ethanol in a round flask equipped with a magnetic stirring rod and spherical condenser. After stirred for 30 min, the solution was heated to a predetermined temperature and a certain amount of Silane69 (commercial grade) was added (0.002 mol per 1 g of ceramic powder). Then the reaction was maintained for 6 hours at $50\,\mathrm{^{\circ}C}$ temperature. Finally, the product was purified with ethanol, centrifuged and air dried.

The surface modification was confirmed by Fourier-transform infrared spectrometer (Bruker, USA), thermo gravimetric analyzer (SDTQ600, USA), x-ray fluorescence spectrometer and SEM coupled with energy-dispersive X-ray spectrometer (EVOLS15, Germany).

2.3 Preparation of Ceramic Filler Loaded Natural Rubber Composites

All the formulations were mixed using the two roll milling process and the vulcanization was done to prepare the final composites.

2.3.1 Preparation of Natural Rubber (NR) and Ceramic Waste (C125) (particle size \leq 125 μ m) Composites.

Natural rubber based composite materials were prepared with different levels of ceramic filler loadings as shown in Table 1.

Table 1 Compounding formulation for NR+C125 composites sample series

Ingredients	Units = parts per rubber						
Sample ID	S0	S1	S2	S3	S4	S5	S6
NR	100	100	100	100	100	100	100
C125	0	5	25	50	75	100	125
ZnO	5	5	5	5	5	5	5
Stearic acid	2	2	2	2	2	2	2
TBBS	2	2	2	2	2	2	2
TMTD	0.1	0.1	0.1	0.1	0.1	0.1	0.1
IPPD	0.5	0.5	0.5	0.5	0.5	0.5	0.5
Sulphur	2.5	2.5	2.5	2.5	2.5	2.5	2.5
Processing oil	7.5	7.5	7.5	7.5	7.5	7.5	7.5

2.3.2 Preparation of Natural Rubber (NR) and Surface Modified C125 Ceramic Powder with Silane (CS) Composite

Natural rubber based composite materials were prepared with different levels of ceramic filler loadings as shown in Table 2.

 $\textbf{Table 2} \ \textbf{Compounding formulation for NR+CS composites sample series}$

Ingredients	Units = parts per rubber					
Sample ID	S7	S8	S9	S10	S11	S12
NR	100	100	100	100	100	100
CS	5	25	50	75	100	125
ZnO	5	5	5	5	5	5
Stearic acid	2	2	2	2	2	2
TBBS	2	2	2	2	2	2
TMTD	0.1	0.1	0.1	0.1	0.1	0.1
IPPD	0.5	0.5	0.5	0.5	0.5	0.5
Sulphur	2.5	2.5	2.5	2.5	2.5	2.5
Processing oil	7.5	7.5	7.5	7.5	7.5	7.5

2.4 Evaluation of Mechanical Properties of the Composites

All the prepared composites were vulcanized and test pieces were prepared using required standards.

2.4.1 Determination of Tensile Properties

The tensile properties of samples were determined by a Tensometer (Instron 3300, USA) material testing machine at a crosshead speed of 500 mm/min according to ISO 37: 2011 standards. All the tests were carried out at 27 \pm 2 °C. Dumbbell shaped specimens was punched out using the tensile cutter. Manual thickness gauge was used to measure the thickness of the narrow portion of tensile pieces. The samples were held tight by the two grips or jaws of the Tensometer, the lower grip was being fixed. The tensile strength, elongation at break and modulus were determined by the Tensometer. Each measurement was evaluated using five test pieces and statistical averages were reported.

2.4.2 Determination of Tear Strength

The tear test was done using the Tensometer (Instron 3300, USA) according to ISO 34-1: 2011 standards. All the tests were carried out at 27 \pm 2 °C. Crescent-shaped test pieces were cut from 2 mm thickness sheets. Then the specimen was placed on the grips of the testing machine and pulled at a rate of 50 mm/min until rupture. Four test pieces were used and average value was determined.

2.4.3 Determination of Hardness

The hardness of the molded samples was determined using a digital hardness tester (Elastocon, Sweden) according to the ISO 48: 2011(E) standards at 27 ± 2 °C. The tests were performed on unstressed samples of 38 mm diameter and 12 ± 0.2 mm thickness. Readings were taken after 10 seconds from the indentation as IRHD values.

2.4.4 Determination of Abrasion Volume Loss

Abrasion volume loss of the samples were measured using an abrasion tester (Hampden APH 40, England). Test specimens of 15 mm diameter and 8 \pm 0.2 mm thickness were placed on a rotating holder and a 10 N load was applied. A pre run was given for conditioning the sample and the initial sample weight was taken. Weight after the test was also taken. The difference in weight is the weight loss of the test piece after its travel through 40 cm on a standard abrasive surface. All the tests were carried out at 27 \pm 2 °C. Three test pieces were used and average value was calculated.

Abrasion volume loss =
$$\frac{(Initial\ weight - Final\ weight)}{Density} \times 1000$$

2.4.5 Determination of Resilience

The horizontal rebound method according to ISO 4662: 2009R was used to measure the rebound resilience of the samples. According to the method a plunger suspended from a given height above the specimen was released and the rebound height was measured. The resilience scale was marked in 100 equally spaced divisions and hence the rebound height was equal to the resilience percentage. Three test pieces were used and average value was calculated. The rebound resilience test was carried out at room temperature (27 \pm 2 °C).

2.4.6 Determination of Compression Set

Compression set of the test samples were measured by applying a constant load on test pieces for continuous 72 hours using compression set testing apparatus. Three test pieces were used and average value was calculated. The compression test was carried out at room temperature (27 $\pm~2~^\circ\text{C}$). Obtained data were interpreted and analyzed using Microsoft Excel 10.0 and Origin 6.0 software.

2.5 Preparation of ball Milled Ceramic Powder Filler Added Natural Rubber Composites

In order to investigate the effect of the incorporation of reduced particle sized filler in to the natural rubber, it was prepared three different composites with the ball milled sub micrometer sized ceramic powder filler loading of 15, 25 and 50 phr. Other ingredients were added as the exactly same compositions in section 2.3. The mechanical properties were tested for these composites as mentioned in section 2.4.

3. Results and Discussion

3.1 Preparation of Ceramic Waste Powder

Fourier transform infra-red (FTIR) spectra of KBr pellets prepared from this initial ceramic powder (Fig. 1) were obtained using Alpha FTIR spectrophotometer (Bruker, USA).

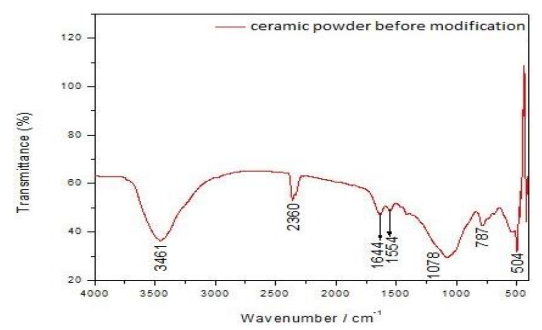


Fig. 1 FTIR spectra of the ceramic powder before modification

Fig. 1 shows the FTIR spectra of the initial ceramic waste powder and it is shows that major absorption bands are in good agreement with the reported values of SiO_2 (Table 3) [20].

Table 3 FTIR absorption bands of initial ceramic powder with band assignments and reported bands of SiO_2 pristine sample [20]

Bonding vibration modes	Corresponding Wavenumber (cm ⁻¹)		
	Actual SiO ₂	Ceramic powder	
Si-O Asymmetric bending	450-510	504	
Si-O-Si Symmetric stretching	800-820	785	
Si-O-Si Asymmetric stretching	1000-1260	1078	
Combined vibrations of the SiO ₂ network	1640, 1870, 1960	1644,1554	
OH stretching - due to surface OH	3000-40000	3481	

These FTIR results indicates that the composition of initial ceramic powder is much similar to the SiO_2 as SiO_2 is one of the major ingredients in the ceramic manufacturing process. Elemental analyses and composition of the phases of these initial ceramic particles were determined by X-ray fluorescence spectroscopy (Fig. 2, Table 3) and X-ray diffraction techniques (Fig. 3) respectively.

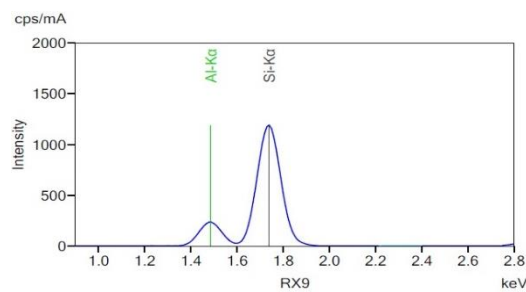


Fig. 2 X-ray fluorescence spectroscopy of initial ceramic powder

Table 4 Elemental data obtained form XRF for initial ceramic sample

Element	Compound	Mass %
Si	SiO ₂	60.3
Al	Al_2O_3	20.2
Na	Na ₂ O	9.06
K	K ₂ O	3.98
Fe	Fe_2O_3	2.35
Ti	TiO ₂	0.83

According to the XFR spectrum (Fig. 2) Si-K α and Al-K α lines represent Si and Al as the major constituents in the initial ceramic powder. According to the Table 4, Si present as SiO₂ is in the mass percentage of 60.3% and Al present as Al₂O₃ is in the mass percentage of 20.2%. Elements like Na, K, Fe and Ti are present as minor constituents in the initial ceramic powder.

Fig. 3 shows the X-ray diffractograms (XRD) of the initial ceramic sample. The peaks corresponding to the (111), (220), and (311) planes could indicate the presence of clusters of silicon. The result reveals that a high percentage of these particles are amorphous, but a few of them are crystalline.

The average particle size and the surface morphology of the initial ceramic powder were investigated using scanning electron microscopic (SEM) techniques (Fig. 4).

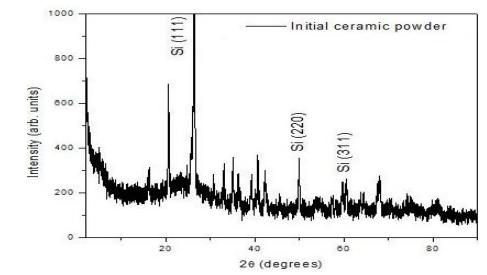


Fig. 3 X-ray diffractograms of initial ceramic powder

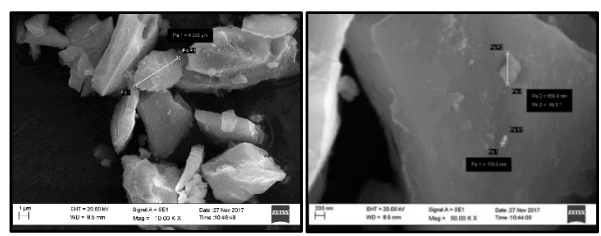


Fig. 4 Scanning electron microscope images of initial ceramic powder (a) under $10000 \times$ magnification (b) under $50000 \times$ magnification

The SEM micrograph indicates the prepared initial ceramic powder is irregular in shape and size. The morphology is rough in all the samples. The particle sizes are between 125 μm and below.

The elemental composition present in the initial ceramic powder was further identified by the energy-dispersive X-ray spectroscopy (Fig. 5, Table 5) coupled with SEM.

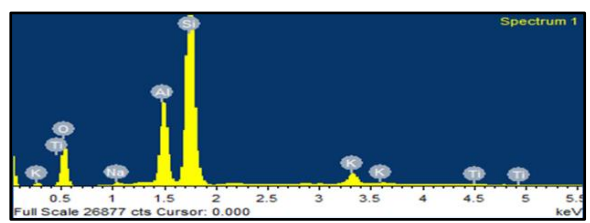


Fig. 5 Energy-dispersive X-ray spectrum of the initial ceramic powder

Energy-dispersive X-ray spectroscopy results suggest the presence of Si and oxygen elements, confirming the presence of SiO₂ particles. The SiO₂ compound percentage is found as much higher 77.15% which is according to the Table 5. Also Al also present in the form of Al₂O₃ and having the compound percentage of 18.47%. Elements like Al, Na, K, Fe and Ti are found as minor constituents.

 $\textbf{Table 5} \ \ \textbf{Elemental composition of the initial ceramic powder obtained from the energy-dispersive x-ray spectroscopy}$

		• •			
Element	Weight%	Atomic%	Compound%	Formula	
Si	36.06	26.16	77.15	SiO ₂	
0	50.70	64.58	-	-	
Al	9.77	7.38	18.47	Al_2O_3	
K	2.30	1.20	2.77	K_2O	
Na	0.47	0.41	0.63	Na_2O	
Fe	0.46	0.17	0.60	FeO	
Ti	0.24	0.10	0.40	TiO ₂	

3.2 Surface Modification of Ceramic Particles

The surface modification was carried out by Silane69 coupling agent. After the chemical procedure of the surface modification by Silane69 coupling agent, the modification was confirmed using Fourier-transform infrared spectroscopic results as shown in the Fig. 6.

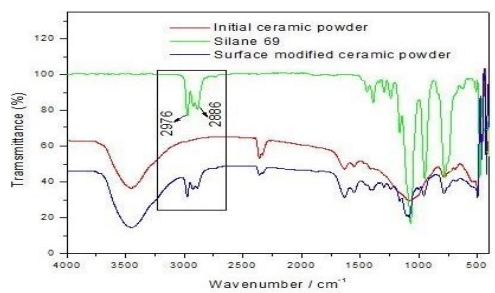


Fig. 6 FTIR spectra of initial ceramic powder, Silane69 and surface modified ceramic powder using silane

In the surface modification process a grafting reaction occurs between the hydroxyl groups from ceramic powder and the silanol groups formed by hydrolysis of the Silane69 coupling agent. Therefore, the grafting reaction between Silane69 and ceramic powder can be identified by the appearance of characteristic bands in FTIR spectra, such as characteristic band of \tilde{v}_{CH2} appearing at 2976–2886 cm $^{-1}$. Fig. 6 shows FTIR spectra of ceramic powder, Silane69 grafted ceramic powder and Silane69. It can be seen that the \tilde{v}_{CH2} band exists in Silane69 grafted ceramic powder, which is the evidence that Silane69 molecules are grafted on the ceramic powder surface and the surface has been modified.

The surface modification caused by Silane69 coupling agent was further confirmed by X-ray fluorescence spectroscopy (Fig. 7, Table 6).

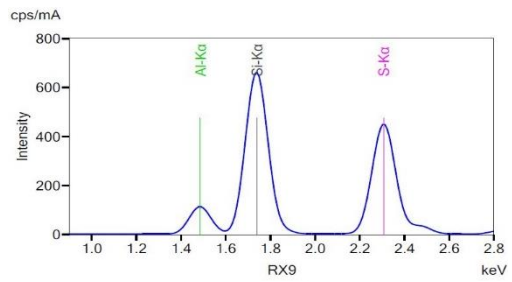


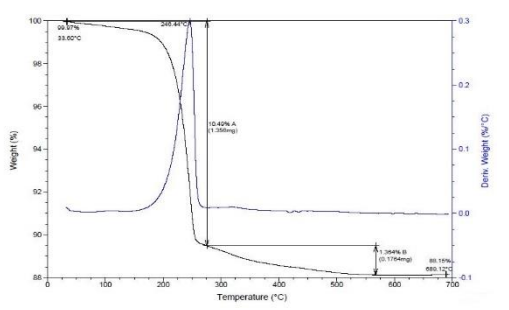
Fig. 7 X-ray fluorescence spectroscopy of surface modified ceramic powder using Silane69

According to the XFR spectrum (Fig. 7) Si-K α and Al-K α lines represent Si and Al as the major constituents as in the initial ceramic powder (Fig. 2). Instead of them S-K α line is present in the spectrum that indicates S as a major constituent in the surface modified ceramic powder. According to the Table 6, Si present as SiO₂ is in the mass percentage of 43.1%, Al present as Al₂O₃ is in the mass percentage of 14.8% and S present in the mass percentage of 9.18%. Na, K, Fe, Ti are present as minor constituents in the surface modified ceramic powder.

 $\textbf{Table 6} \ \ \textbf{Elemental data obtained form XRF for surface modified ceramic powder using Silane 69}$

Element	Compound	Mass %
Si	SiO ₂	43.1
Na	Na ₂ O	26.4
Al	Al_2O_3	14.8
S	SO_3	9.18
K	K ₂ O	2.52
Fe	Fe_2O_3	1.03
Ti	TiO ₂	0.49

The surface modification caused by Silane69 coupling agent was further confirmed by thermo gravimetric analysis (TGA) (Fig. 8).



 $\textbf{Fig. 8} \ \text{Thermo gravimetric curve of surface modified ceramic powder using Silane 69}$

TGA of surface modified ceramic powder using Silane69 (Fig. 8) shows gradual weight loss at 246.44 °C (10.49%). This weight loss may be due to removal of free water absorbed from atmosphere and presence of any structural water. Gradual weight loss from 250 °C to 550 °C (1.364%) is due to dihydroxylation for structural OH. This confirms the surface modification of ceramic powder by Silane69.

The surface modified ceramic powder were subsequently analyzed by scanning electron microscopy (SEM). The SEM micrographs of surface modified ceramic powder (Fig. 9) confirmed our speculation. From SEM, pristine initial ceramic particles (Fig. 4) presented irregular shaped and rough morphology and small aggregates could be observed due to hydrogen bonds between the surface hydroxyl groups of silica particles. After silane grafting, the surface modified particles show regular spherical structure. The modified particles have sticked to each other and formed large aggregations after silane modification. Also the surface morphology

of modified ceramic particles looks smooth and sleek compare to the pristine initial ceramic particle morphology.

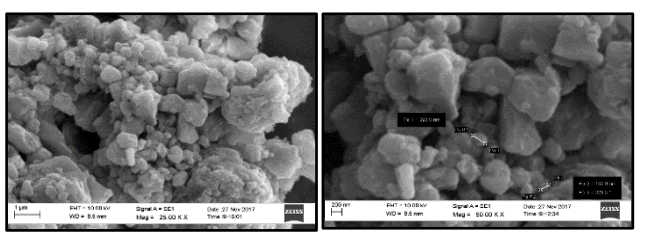


Fig. 9 Scanning electron microscope images of surface modified ceramic powder (a) under $25000 \times$ magnification (b) under $50000 \times$ magnification

The Silane69 coupling agent which was used for the surface modification is composed of C, O, H, S and Si in its chemical structure (Fig. 10).

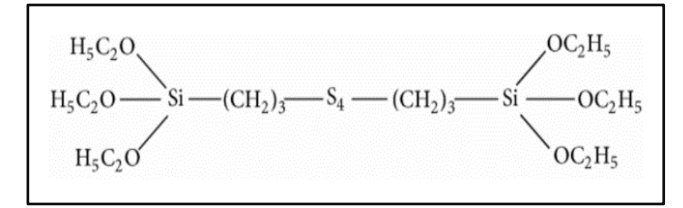
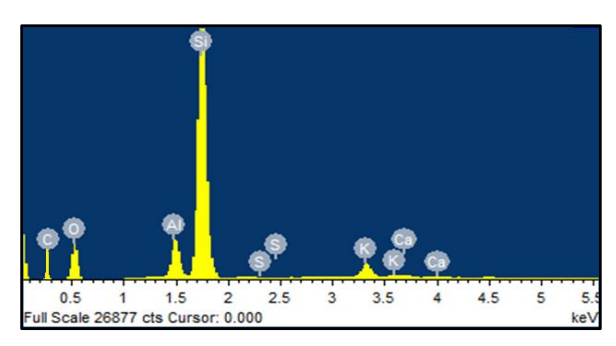


Fig. 10 Chemical structure of Silane69 coupling agent

So the surface modification can be further confirmed by examining the elemental composition present in the surface modified ceramic powder using energy-dispersive x-ray spectroscopy (Fig. 11, Table 7) coupled with SEM.



 $\textbf{Fig. 11} \ \textbf{Energy-dispersive} \ \textbf{x-ray} \ \textbf{spectrum} \ \textbf{of the surface} \ \textbf{modified ceramic} \ \textbf{powder}$

Energy-dispersive X-ray spectroscopy results suggest the surface modification of ceramic particles with the excess presence of C and S elements, compare to the pristine initial ceramic powder (Table 5).

Table 7 Elemental composition of the surface modified ceramic powder obtained from the energy-dispersive X-ray spectroscopy

Element	Weight%	Atomic%	Compound%	Formula
Si	29.53	19.34	63.17	SiO ₂
0	57.19	65.77	-	-
С	7.54	11.55	27.63	CO_2
Al	3.17	2.16	5.99	Al_2O_3
K	1.99	0.94	2.40	K ₂ O
Ca	0.27	0.12	0.38	CaO
Fe	0.27	0.09	0.35	FeO
S	0.03	0.02	0.08	SO_3

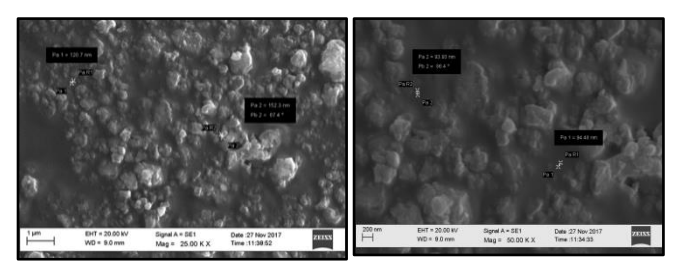


Fig. 12 Scanning electron microscope images of ball milled ceramic powder (a) under $25000 \times$ magnification (b) under $50000 \times$ magnification

3.3 Preparation of Sub Micrometer Sized Ceramic Waste Powder

Initially prepared ceramic waste powder was ball milled for 6 hours at an 800 rpm speed by a laboratory planetary ball mill followed by dry milling. The average particle size and the surface morphology was characterized by scanning electron micrographs (Fig. 12).

The SEM micrograph indicates the ball milled ceramic powder is irregular in shape and size. The particle sizes are between few nm to few hundred nanometers. The particle size has become smaller compared to the pristine initial ceramic powder sample with the effect of ball milling. Particle aggregations also can be observed up to some extent.

X-ray diffraction pattern shows the crystalline structure the ball milled ceramic powder (Fig. 13). Typical silica characteristic is observed with an intense sharp peak centered at 2θ = 26° . Reduction in crystallite size is observed with the effect of ball milling.

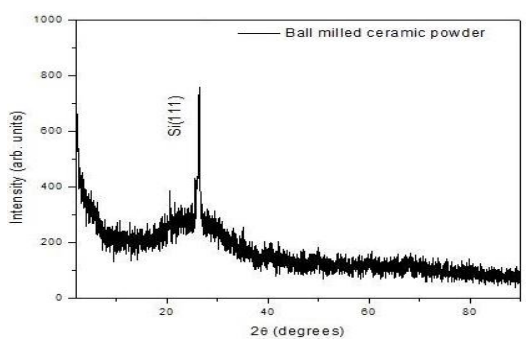


Fig. 13 X-ray diffractograms of ball milled ceramic powder

3.4 Mechanical Property Comparison of Surface Modified and Non-Modified Ceramic Powder Filler Added Natural Rubber Composites

3.4.1 Tensile Strength

Tensile strength of ceramic filler containing composites is higher than that of the pristine rubber composite (control) up to 50 phr filler loading. At higher filler loadings (75 phr), tensile strength is lower than that of the control and could be attributed to agglomeration of filler particles. Surface modified ceramic filler loaded composites have higher tensile strength than non-modified ceramic filler loaded composites at some of the filler loadings (Fig. 14).

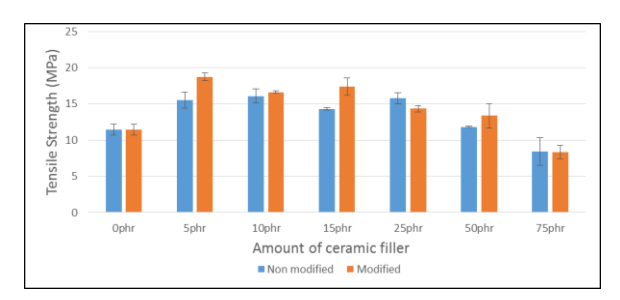


Fig. 14 Tensile strength comparison of surface modified and non-modified ceramic powder filler added natural rubber composites

3.4.2 Modulus at 100% Elongation

Modulus at 100% elongation is related to hardness or stiffness of the composites. As in the case of hardness, modulus at 100% elongation of ceramic filler loaded composites is higher than that of the control. However, no significant difference is observed between the modulus at 100% elongation of surface modified ceramic filler loaded composites and non-modified ceramic filler loaded composites (Fig. 15).

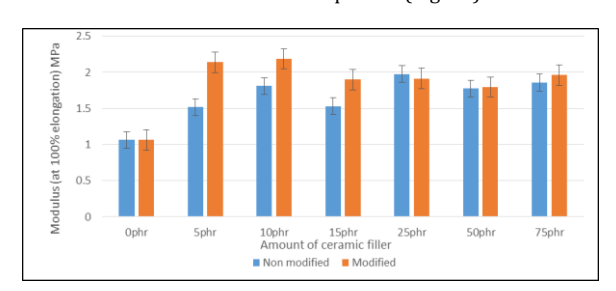


Fig. 15 Modulus at 100% elongation comparison of surface modified and non-modified ceramic powder filler added natural rubber composites

3.4.3 Elongation at Break

As expected, elongation of the control is higher than that of the ceramic filler containing composites. Elongation at break of the surface modified ceramic filler loaded composites is higher than that of non-modified ceramic filler loaded composites at filler loadings 50 phr and above (Fig. 16).

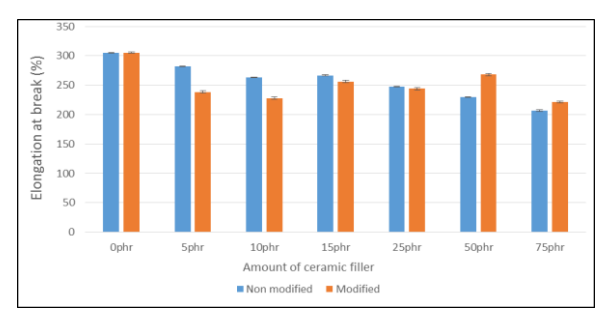


Fig. 16 Elongation at break comparison of surface modified and non-modified ceramic powder filler added natural rubber composites

3.4.4 Tear Strength

Tear strength of ceramic filler loaded composites is lower than that of the control. As in the case of elongation at break, tear strength of surface modified ceramic filler loaded composites is higher than that of non-modified ceramic filler loaded composites at filler loadings 50 phr and above (Fig. 17).

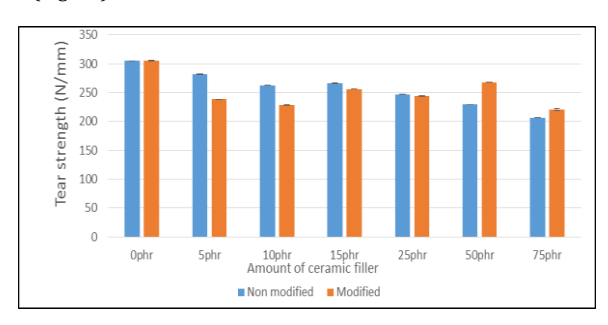


Fig. 17 Tear strength comparison of surface modified and non-modified ceramic powder filler added natural rubber composites

3.4.5 Hardness

As expected, hardness increases with the increase of ceramic filler loading. Surface modified ceramic filler containing composites have lower hardness than non-modified ceramic filler containing composites at 25 phr loading and above (Fig. 18).

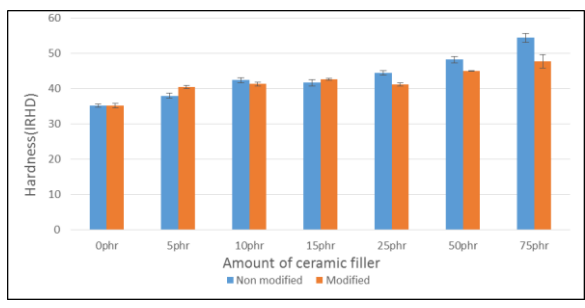


Fig. 18 Hardness comparison of surface modified and non-modified ceramic powder filler added natural rubber composites

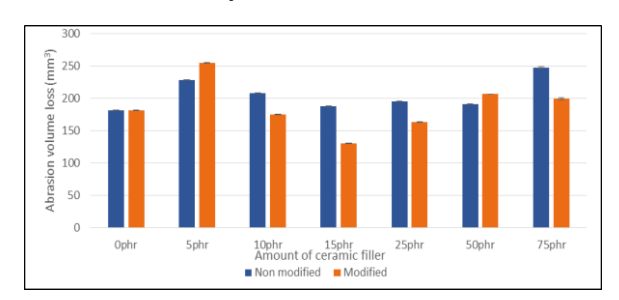


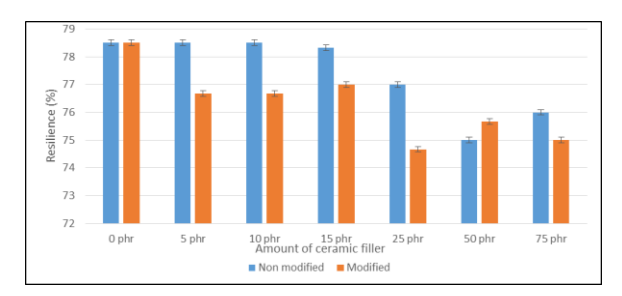
Fig. 19 Abrasion volume loss comparison of surface modified and non-modified ceramic powder filler added natural rubber composites

3.4.6 Abrasion Volume Loss

Abrasion volume loss of the composites varies with the ceramic filler loading according to a cyclic pattern. At most of the ceramic filler loadings, surface modification has resulted in a decrease in the abrasion volume loss (Fig. 19).

3.4.7 Resilience

Resilience of ceramic filler loaded composites is lower than that of the control except at 5 phr and 10 phr non –modified filler added composites. Resilience gets decrease with the increasing amount of filler added. Resilience of non-modified filler added composites is larger than modified filler added composites except at 50 phr filler loading (Fig. 20).



 $\textbf{Fig. 20} \ \ Resilience \ \ (\%) \ \ comparison \ \ of surface \ modified \ and \ non-modified \ ceramic \ powder \ filler \ added \ natural \ rubber \ composites$

3.4.8 Compression Set

Compression set of the composites decrease with the ceramic filler loadings compared to the control. Surface modified composites have little lower compression set compared to non-modified composites. Compression set is increasing after 15 phr filler loadings and this may cause due to agglomerations (Fig. 21).

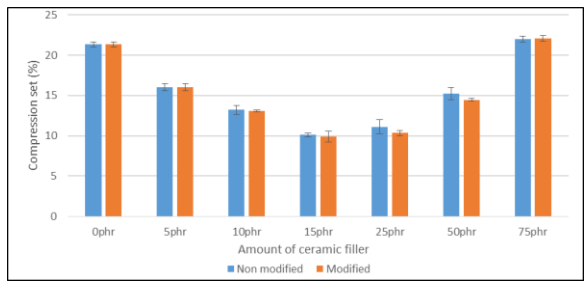


Fig. 21 Compression set (%) comparison of surface modified and non-modified ceramic powder filler added natural rubber composites

Due to the addition of fillers, molecular chain mobility is decreasing with time. Up to some extend ceramic fills the void spaces between natural rubber. So that hardness, compression resistance, 100%modulus, tensile strength like properties gets increased. With the higher filler adding insufficient sites of natural rubber is increasing. So that above properties get decreased (Fig. 22).

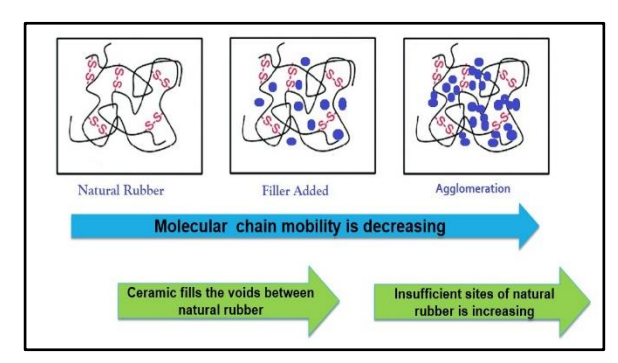


Fig. 22 Explanation of obtained mechanical properties

3.5 Mechanical Properties of Ball Milled Ceramic Powder Filler Added Natural Rubber Composites

In this experiment ceramic filler added natural rubber composites were made in 0, 5, 10, 15, 25, 50 and 75 phr compositions. It was found to have these composites show the optimal properties at moderate compositions. In order to investigate the effect of the incorporation of reduced particle sized filler in to the natural rubber, it was prepared three different

composites with the ball milled sub micrometer sized ceramic powder filler loading of 15, 25 and 50 phr.

When it compares the modulus at 100% elongation of the ball milled sub micrometer sized ceramic filler added composites with the initial nonball milled ceramic filler added composites, it was found to have much improved modulus can be achieved by reduced particle size filler loadings due to the dense packing. Optimal mechanical properties can achieve by adding less loading of ball milled ceramic particles compared to non-ball milled ceramic particles (Fig. 23). This may due to the ability of ball milled ceramic particles that they tend to fill the void spaces of natural rubber matrix more than that of the non-ball milled ceramic particles.

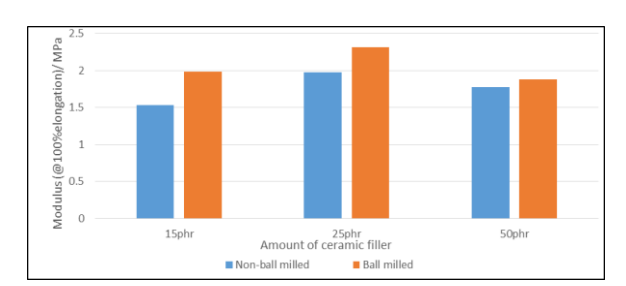


Fig. 23 Modulus at 100% elongation comparison of ball milled and non-ball milled ceramic powder filler added natural rubber composites

4. Conclusion

Ceramic waste are the kind of major wastes in manufacturing sectors. The aim of this investigation was the utilization of these ceramic waste as a low cost filler material in the manufacture of natural rubber based composites. Mechanical properties of ceramic waste-based natural rubber composites have been investigated as a function of fiber loading, ratio and treatment. The surface modification it was found that the incorporation of ceramic waste filler enhanced the mechanical properties of the natural rubber. As the filler concentration increases, the modulus at the 100%elongation and tensile strength slightly increased, but the elongation at break decreased may due to reinforcing effects. The hardness was also found to increase with the loading level of ceramic waste in the composites. This is due to the increased material stiffness. These composites also found to have better compression resistant compared to the pristine natural rubber. The filler surface modification with Silane69 coupling agent further improved the mechanical properties of composites. Furthermore, optimal mechanical properties can achieve by adding less loading of ball milled ceramic particles compared to non-ball milled ceramic particles. Overall, the mechanical performance of the ceramic waste based natural rubber composites was better than that of the control. It was observed that the optimal mechanical properties of the composites are present at moderate loading of fillers. Pristine natural rubber compound shows low mechanical properties such as; low hardness, low modulus at 100% elongation and low tensile strength. Compared to that these novel ceramic waste based natural rubber composites shows improved mechanical properties such like; compression resistant, high hardness, high modulus and high tensile strengths. Finally, it can be concluded that, within the limited scope of the experiments carried out in this investigation, these ceramic waste based natural rubber composites can be utilized as a proper flooring material.

Acknowledgments

The authors thank Uva Wellassa University of Sri Lanka for partial financial support provided under the grant number UWU/RG/2016/11. A portion of this research used resources at Instrument Center operated by Faculty of Applied Sciences of University of Sri Jayewardenepura, Center of Advance Material Research at University of Sri Jayewardenepura and Rubber Research Institute of Sri Lanka. The authors greatly acknowledged the support given by those facilities to make this work success.

References

- D. Hoornweg, P. Bhada-Tata, What a waste: a global review of solid waste management, World Bank, Washington DC, 2012.
- [2] S.K. Amin, H.A. Sibak, S.A. El-Sherbiny, M.F. Abadir, An overview of ceramic wastes management in construction, Int. J. Appl. Eng. Res. 11(4) (2016) 2680-2685.
- [3] P.B. Vyas, Assessment of municipal solid waste compost characterization and compliance, J. Ind. Pollut. Control. 27(1) (2011) 87-91.

- [4] I.B. Topcu, M. Canbaz, Utilization of crushed tile as aggregate in concrete, Iran J. Sci. Technol. Trans. B. Eng. 31 (2007) 561-565.
- [5] P. Torkittikul, A. Chaipanich, Utilization of ceramic waste as fine aggregate within Portland cement and fly ash concretes, Cem. Concr. Compos. 32(6) (2010) 440-449.
- [6] A. Halicka, P. Ogrodnik, B. Zegardlo, Using ceramic sanitary ware waste as concrete aggregate, Constr. Build. Mater. 48 (2013) 295-305.
- [7] J. Jimenez, J. Ayuso, M. Lopez, J. Fernandez, J. Brito, Use of fine recycled aggregates from ceramic waste in masonry mortar manufacturing, Constr. Build. Mater. 40 (2013) 679-690.
- [8] J. Brito, A. Pereira, J. Correia, Mechanical behavior of non-structural concrete made with recycled ceramic aggregates, Cem. Concr. Compos. 27(4) (2005) 429-433.
- [9] L. Pereira-de-Oliveira, J.C. Gomes, P. Santos, The potential pozzolanic activity of glass and red-clay ceramic waste as cement mortars components, Constr. Build. Mater. 31 (2012) 197-203.
- [10] C. Medina, M. Frias, M. Sanchez de Rojas, Microstructure and properties of recycled concretes using ceramic sanitary ware industry waste as coarse aggregate, Constr. Build. Mater. 31 (2012) 112-118.
- [11] B. Erman, J. Mark, C. Roland, The science and technology of rubber, 4th Ed., Elsevier, Waltham, 2013.
- [12] L. Vaysse, F. Bonfils, J. Sainte-Beuve, M. Cartault, Natural rubber: Polymer science: A comprehensive reference, Elsevier, Waltham, 2012.

- [13] C.H. Chan, J. Joy, J. Maria, Natural rubber-based composites and nanocomposites: State of the art, new challenges and opportunities, Nat. Rubber. Mater. 1 (2013) 1-27.
- [14] J.W. Brinke, S.C. Debnath, L.A.E.M. Reuvekamp, J.W.M. Noordermeer, Mechanistic aspects of the role of coupling agents in silica-rubber composites, in: R.P. Hjelm, M. Gerspacher, A. le Mehaute, R. Schuster, F. Tsobnang (Eds.), Composites science and technology, Elsevier, Kidlington, Oxford UK, 2003, pp.1165-1174.
- [15] Y. Xie, C. Hill, Z. Xiao, H. Militz, C. Mai, Silane coupling agents used for natural fiber: polymer composites: A review, Appl. Sci. Manu. 41(7) (2010) 806-819.
- [16] W. He, D. Wu, J. Li, K. Zhang, Y. Xiang, L. Long, Surface modification of colloidal silica nanoparticles: Controlling the size and grafting process, Bull. Korean. Chem. Soc. 34(9) (2013) 2747–2752.
- [17] Q. Zhang, M. Tian, Y. Wu, G. Lin, L. Zhang, Effect of particle size on the properties of Mg(OH)₂-filled rubber composites, J. Appl. Polym. Sci. 94(6) (2004) 2341-2346.
- [18] T. Ahmad, O. Mamat, The development and characterization of zirconia-silica sand nanoparticles composites, World J. Nano Sci. Eng. 1(1) (2011) 7-14.
- [19] T. Yokoyama, Y. Taniyama, G. Jimbo, Q. Zhao, The grinding equilibrium size of in-water grinding of silica sand by a planetary ball mill, Adv. Powder. Technol. 28(12) (1991) 751-758.
- [20] R. Ullah, B.K. Deb, M. Yousuf, A. Mollah, Synthesis and characterization of silica coated iron-oxide composites of different ratios, Int. J. Compos. Mater. 4(2) (2014) 135–145.